ADVANCED ENGINEERING MATERIALS
www.aem-journal.com

Scalable Manufacturing of Polymer Multi-Nanofiber Twisted Yarns

*Mohamad Keblawi, Adaugo Enuka, Darrian Shufford, and Vince Beachley**

Continuous high-strength polymer nanofiber yarns can be assembled into textiles suitable for numerous applications that benefit from the high surface-area-to-volume ratio of the component nanofibers. Electrospun nanofibers have been used to make multifiber twisted yarns (MFTYs). Traditionally, electrospun nanoyarns are made using self-bundling methods or cone spinning. However, these approaches inhibit ordered fiber architecture or postprocessing of filaments prior to yarn fabrication limiting yarn length, uniformity, and mechanical strength. A spinning process utilizing automated parallel track collection is capable of manufacturing MFTYs with microarchitecture control and integration of individual fiber post-drawing prior to yarn assembly. The advantage of this process is the ability to optimize electrospinning parameters, postprocessing parameters, and yarn spinning parameters independently. Polycaprolactone (PCL) fibers are electrospun with various parameters and made into long MFTYs that retain up to 50% of the strength of individual component nanofibers. Mechanical testing shows relationships between spinning parameters and yarn strength. The tenacity of PCL MFTYs exceeds the tenacity of most reported self-bundled nanofiber yarns by an order of magnitude or more. Thus, the alternative nanoyarn fabrication method presented in this work is able to produce yarns with highly tunable parameters with a significant increase in mechanical strength compared to other electrospun nanoyarns.

1. Introduction

Yarn can be classified either as staple yarns or continuous filament yarns.[1] Continuous filament yarns are made by extruding a polymer solution or melt through a spinneret, which solidifies into a solid fiber through solvent evaporation or cooling, respectively.[2] The extrusion process is capable of forming continuous filament with lengths of hundreds of meters, which can be twisted to form continuous filament yarns.[3] Staple yarns on the other hand are made by twisting short fiber segments.[4] The friction forces between the short fiber segments allow staple yarns to resist forces without unraveling.[5] Thus, staple yarn can also be manufactured to lengths of hundreds of meters, even though the component fiber length is much shorter. The major distinguisher between staple and filament yarns is the length of the fibers that make up the yarn. Cotton and wool staple yarns are composed of fibers with lengths falling between 25 mm and 150 mm.[6] Filament yarns on the other hand are composed of fibers that have an indefinite length up to hundreds of meters. Yarns fabricated using the proposed method are structurally similar to staple yarns, but the component fiber length could be between 10 and 400 mm,[7] so they will be referred to as multifiber twisted yarns (MFTYs) as their fiber component length may exceed 150 mm. A yarn's structure is held by a combination of the strength of its component fibers, as well as the riction between said fibers. More often than not, mechanical failure in yarns occurs due to slippage between its component fibers. One way to assess the mechanical performance of a yarn is to divide the specific strength of the yarn by the specific strength of an individual component fiber. This is referred to as the yarn-to-fiber strength ratio. For example, the yarn-to-fiber strength ratio of cotton staple yarns ranges between 30 and 40%.[8]

Interest in nanofiber technologies and their applications has been evident in previous years.[9] This is due to their high surface-area-to-volume ratio, which provides a theoretical rationale for unique and/or enhanced mechanical strength, electrical and thermal conductivity, optical properties, and sensing and filtration capabilities as compared to their microscale counterparts.[10] Electrospinning is a popular method of nanofiber production. This is due to its relative ease to setup, low cost, and its ability to produce nanofibers from a wide range of polymers.[11] The advantages of nanofibers as well as the ease of setup and low cost of electrospinning have allowed for the use of electrospun nanofibers in many applications, notably, tissue engineering, filtration, and energy storage.[12–15] Electrospinning can also be used to make nanofiber yarns using a self-bundling approach.[16] Self-bundling nanoyarn production is typically done by electrospinning two or more oppositely charged jets. The oppositely

M. Keblawi, D. Shufford, V. Beachley
Department of Biomedical Engineering
Rowan University
Glassboro, NJ 08028, USA
E-mail: beachley@rowan.edu

A. Enuka, V. Beachley
Department of Chemical Engineering
Rowan University
Glassboro, NJ 08028, USA

The ORCID identification number(s) for the author(s) of this article can be found under https://doi.org/10.1002/adem.202401897.

DOI: 10.1002/adem.202401897

charged fibers self-bundle, in air, into yarns that are twisted and rolled onto a take-up mandrel. This approach was then improved by adding an electrically grounded and spinning cone.[16–18] The cone serves as a location for fiber deposition and imparts ordered fiber orientation. As mentioned earlier, one of the characteristics of all self-bundling approaches is that both fiber electrospinning and yarn spinning occur simultaneously. This means that post-processing of fibers cannot be performed prior to spinning them into the yarn. The self-bundling approach also limits the range of linear density of the resulting yarn because a minimum solution pump rate is required for electrospinning to occur, and fiber must be cleared from the deposition area at a certain rate to avoid disruption to the electrospinning process.[19] Additionally, the random nature of electrospinning results in yarns with limited control over fiber alignment. Alternating current (AC) electrospinning can be used to fabricate nanofiber yarns with little modification to the setup.[20,21] AC nanofiber yarn electrospinning is also mediated through a self-bundling process and is subject to the same limitations listed above. Despite intense interest, self-bundling and spinning cone approaches have shown limited success in producing yarns with sufficient mechanical strength, length, and uniformity for commercial production.

Postdrawing of individual electrospun nanofibers using the parallel track manufacturing approach has been shown to improve their mechanical strength with an increasing draw ratio (DR).[22–24] For example, it has been demonstrated that the ultimate tensile strength (UTS) of electrospun polycaprolactone (PCL) nanofibers was increased by seven times when postdrawn to a DR of four (DR4)[25] If strong aligned nanofibers can be spun into ordered MFTY, then the fabrication of desirable nanofiber textiles would be possible.

Previous electrospun nanoyarns have almost exclusively been manufactured with self-bundling or spinning cone approaches. This is due to the difficulty of handling nanofibers postspinning. This article proposes a method of fabricating MFTY using a parallel track device to produce highly aligned nanofibers with different DRs. For yarn production, a roll-to-roll collection system was implemented into the parallel track system (**Figure 1**A,B).

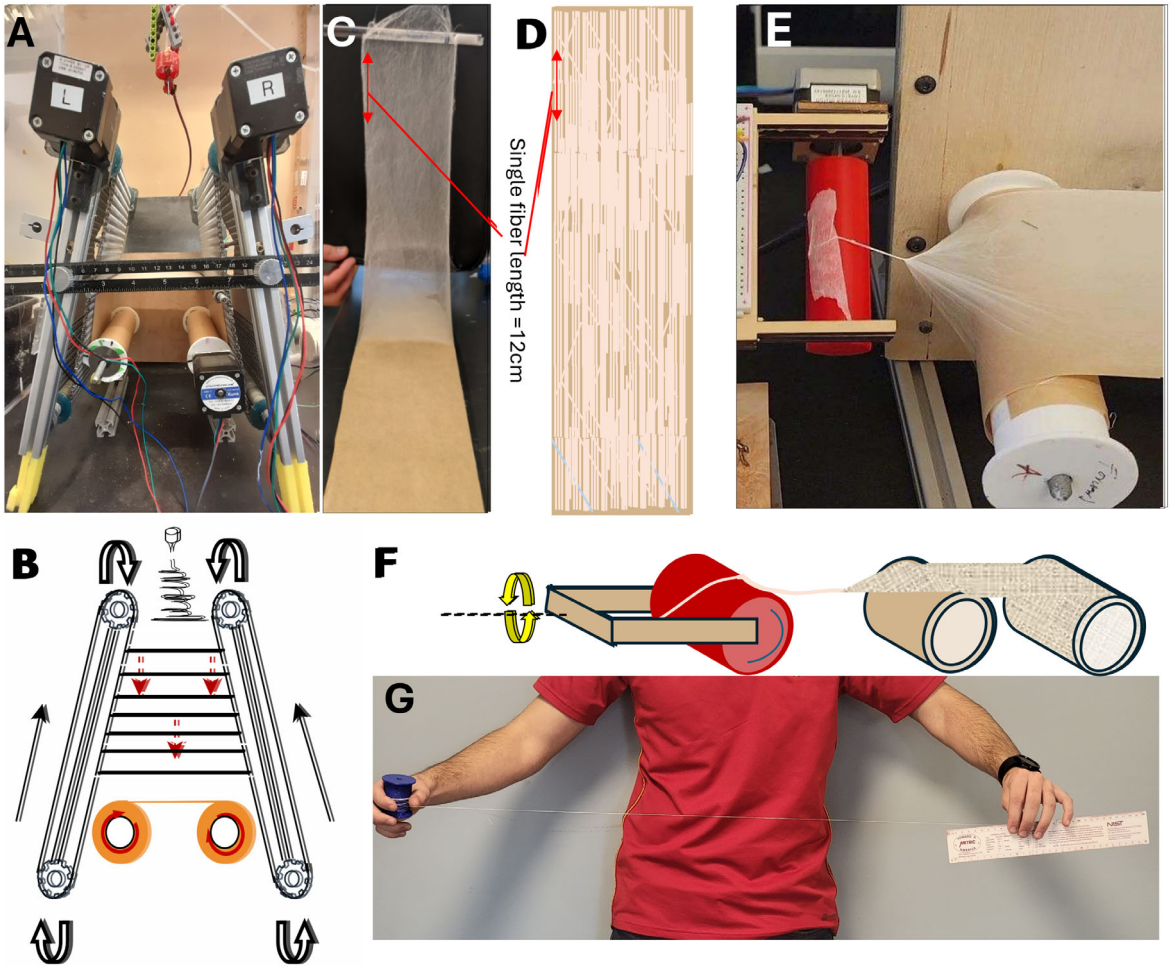

Figure 1. A) Electrospinning setup consisting of aligned discrete length fiber deposition across parallel tracks, which are postdrawn and transferred to a collection roll. B) Schematic diagram of electrospinning device. C) Nanofiber collection roll. Discrete fiber segments with a length of 12 cm are deposited on the collection roll via the parallel track system. D) Schematic diagram showing collected aligned PCL fibers overlapping on roll backing. E) Yarn spinning device twisting and winding a fiber "roving" into a yarn. F) Schematic diagram of yarn spinning device. G) Resulting PCL multifiber twisted yarn. One meter of yarn shown unwound from a 5 meter spool. A 30 cm long ruler is held for scale.

The purpose of this "roving" roll is to collect overlapping, aligned nanofibers over continuous lengths (Figure 1C,D). The roll is then fed into a yarn spinning device (Figure 1E,F) which processes the aligned overlapping fibers into a yarn (Figure 1G). The device consists of a twisting motor that twists the aligned filaments into a yarn and a take-up motor that winds the yarn on a bobbin. The device is capable of controlling the twists per inch (TPI), and thus the twist angle of the resulting MFTY yarn.

This study aims to demonstrate the feasibility of producing long multi-nanofiber twisted yarns with high strength ratios and to study the effect of varying the fiber and yarn spinning parameters on the mechanical properties of the yarns.

2. Experimental Section

2.1. Filament and Yarn Spinning

PCL fibers were electrospun using the device shown in Figure 1A and previously described.[7] The approach consists of an electrospinning system positioned over a device with two parallel tracks that collect, transport, and postdraw the fibers that align across the top gap between the tracks. The collection tracks transfer the fibers onto a roving roll capable of moving at different speeds. Collected fibers are then spun into a yarn using the device shown in Figure 1C. The yarn spinning device consists of a twisting motor and a take-up motor, equipped with bobbins of different diameters. Video S1, Supporting Information, shows the electrospinning and yarn spinning processes. All DR 1 and DR 2.5 fibers were spun using the following spinning solution, 18% wt/v PCL ($M_W = 115$ kDa, Sigma–Aldrich) dissolved in a 3:1 volume ratio of dichloromethane:dimethylformamide (Sigma–Aldrich). DR4 nanofibers (NDR 4) were spun using the following spinning solution, 16% wt/v PCL ($M_W = 115$ kDa) dissolved in a 3:1 volume ratio of dichloromethane:dimethylformamide. The following parameters remained constant for all test groups: electrospinning voltage of 9 kV, needle height at 10 cm, humidity at 60%, track speed of 1.3 mm s^{-1}, a solution pump rate of 1 mL h^{-1}, and fiber length of 12 cm. Three main testing groups were fabricated to assess how the differences in fiber count (FC), yarn TPI, and fiber DR affected yarn morphological and mechanical properties. FC was varied by changing the speed of the roving roll's motor. TPI was varied by changing the uptake speed and bobbin diameter (This can alternatively be changed by changing the twist-to-uptake speed ratio). DR was varied by changing the length of the gap between the tracks at the point closest to the electrospinning nozzle (D_1), and the length of the gap between the tracks closest to the collection roll (D_2). For DR = 1, $D_1 = D_2 = 12$ cm; DR = 2.5, $D_1 = 4.8$ cm, $D_2 = 12$ cm; and DR = 4, $D_1 = 3$ cm, $D_2 = 12$ cm. The individual effects of each of the three test groups were isolated by fixing all other manufacturing variables. The parameters used to fabricate each sample are summarized in **Table 1**. Fibers were deposited onto a roll of wax paper used as the "roving roll" and were dried at room temperature for 2 days to remove residual solvents prior to yarn spinning. Control fiber filaments, used to test single fiber mechanical properties, were spun as described above and postdrawn to DR = 1, DR = 2.5, or DR = 4.

To visualize filament segments within a yarn, dyed filaments were electrospun and incorporated into yarns. Two separate solutions were made using the following dyes: DiI (1,1′-dioctadecyl-3,3,3′,3′-tetramethylindocarbocyanine) and DiO (3,3′-dioctadecyloxacarbocyanine) (Sigma–Aldrich). Electrospinning parameters remained the same with the exception of adding 1% wt/v of dye per solution. A dyed yarn was made by collecting DiI dyed PCL fibers for 10 min on a roving roll moving at 0.6 mm s^{-1}. The roving roll was temporarily stopped to switch to a DiO solution, which was then electrospun onto the same roving roll moving at the same speed for another 10 min.

Table 1. Summary of yarn test groups parameters.

Test groups		
FC	TPI	DR
Roving roll speed: 0.2 mm s^{-1} (high density)	Roving roll speed: 0.6 mm s	Roving roll speed: 0.6 mm s
TPI: 10	TPI: 20	TPI: 10
DR: 1 ($n = 5$)	DR: 1 ($n = 5$)	DR: 1 ($n = 5$)
Roving roll speed: 0.6 mm s^{-1} (medium density)	Roving roll speed: 0.6 mm s	Roving roll speed: 0.6 mm s
TPI: 10	TPI: 40	TPI: 10
DR: 1 ($n = 5$)	DR: 1 ($n = 5$)	DR: 2.5 ($n = 5$)
Roving roll speed: 1 mm s^{-1} (low density)	Roving roll speed: 0.6 mm s	Roving roll speed: 0.6 mm s
TPI: 10	TPI: 80	TPI: 10
DR: 1 ($n = 5$)	DR: 1 ($n = 5$)	DR: 4 ($n = 5$) * nanofibers spun from 16% solution

2.2. Mechanical Testing

Tensile testing was performed on yarn segments with gauge lengths (GL) of 10 mm or 130 mm using a Shimadzu EZ-SX universal tester, Shimadzu 1 kN capstan yarn grips, and a 100 N load cell (Figure 3B,C). Testing was performed according to the ASTM 2256-21 standard with a strain rate of 25% mm/min of the specimen's GL. Fiber testing was performed under the same strain rate using Shimadzu 500 N flat grips and a 100 N load cell. Low-density arrays of aligned fiber were adhered to 5 × 2 cm plastic frames and then mounted on testing grips shown in Figure 3A. The frame was then cut, and the fibers were tensile tested until failure. The cross-sectional area of the multifiber samples was calculated by counting the total number of fibers per sample and multiplying by the cross section of a single fiber calculated from the fiber diameter. Fiber diameter was measured using scanning electron microscopy (SEM).

2.3. Microscopy and Image Processing

Dyed yarns were imaged using confocal laser scanning microscopy (Nikon ECLIPSE Ti) and undyed yarns were imaged using SEM (FEI Apreo 2). Samples were prepared using a Denton

Vacuum Desk II sputter coater and sputter coated with gold for 30 s. The resulting images were processed using ImageJ.

2.4. Data Analysis and Calculations

Data processing and visualization were performed using NumPy, Pandas, and Matplotlib python libraries, as well as Shimadzu's TRAPEZIUM X. Analysis of variance (ANOVA) and student's *t*-test analysis were performed using the SciPy library. Linear density was calculated by dividing the measured mass of the yarn by its measured length. Tenacity was calculated by dividing the maximum measured force by the calculated linear density. UTS was calculated by multiplying tenacity by the volumetric density of PCL. FC per cross section was estimated by dividing the yarn linear density over the fiber linear density. Fiber linear density was estimated by using the measured fiber diameter and assuming the density of PCL fibers to be the bulk density of PCL = 1.145 g cm^{-3}.

3. Results

3.1. Morphology

3.1.1. Individual Fibers

Individual fibers with DR = 1 had an average diameter of 1800 nm, while fibers with a DR = 2.5 had an average diameter of 1400 nm. Both sets of fibers were spun using 18% wt/v PCL solution. In order to produce fibers with an average diameter <1 µm, a 16% wt/v PCL spinning solution was used to produce a nanofiber with a DR of 4. Fibers and yarns produced using the 16% wt/v PCL solution will be referred to as NDR 4. NDR 4 fibers had an average diameter of 830 nm. SEM images (**Figure 2**D) showed a uniform diameter throughout the fiber length and the fiber surface appeared smooth for all samples.

3.1.2. Multifiber Twisted Yarns

Figure 2A–C shows SEM images of PCL MFTYs fabricated with various manufacturing parameters. Low FC yarns had a diameter of 0.28 mm, while medium and high FC yarns had diameters of 0.3 mm and 0.65 mm respectively. Yarns with varied TPI were all manufactured with medium FC and DR 1. Yarns with a TPI of 20 had a diameter of 0.175 mm compared to 0.075 mm for 40 TPI yarns and 0.21 mm for 80 TPI yarns. Finally, both DR 2.5 and NDR 4 yarns had an average diameter of 0.24 mm. MFTYs twist angle was measured using SEM with an observed range of 15°–80°. An increase in twist angle was observed as a result of increasing the TPI, while FC and DR had little effect on the twist angle. Visually, lower FC yarns had a rough and uneven outer surface compared to higher FC yarns which looked smoother. Twists were difficult to spot for lower twist yarns but are easier to identify and measure as the twist increased. Finally, there is very little hairiness in the yarns compared to conventional cotton and wool staple yarns.[26]

MFTYs linear density was correlated to the estimated FC per cross section. Yarns with linear density ranging from 54 to 900 deniers were estimated to have a FC ranging from 2047 to 89 367 fibers in the yarn cross section, respectively.

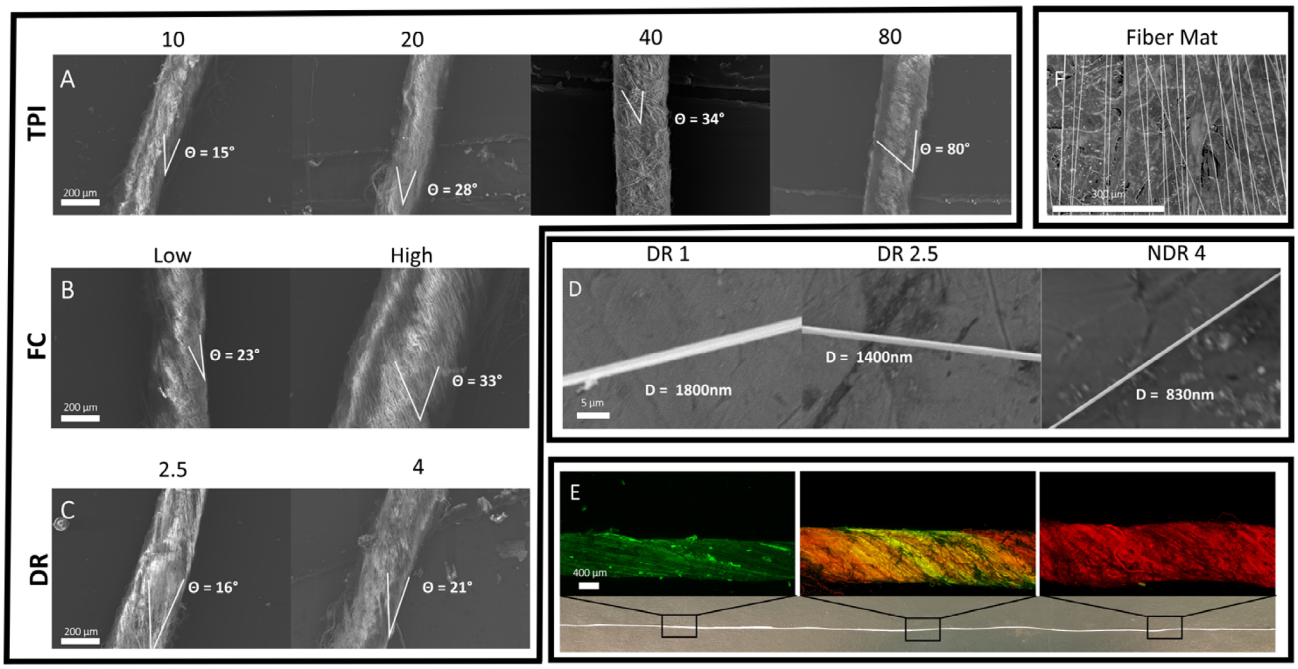

Figure 2. A–C) SEM images of PCL MFTYs, with varied manufacturing parameters: A) TPI, B) FC per cross section, and C) DR. D) Individual fibers of different DRs. E) An MFTY made with the two different types of dyed component fibers with images of differently colored yarn segments corresponding to locations along the length of the yarn. F) Representative image of fibers on the collection roll. All yarns in (A) have a medium FC and DR1, all yarns in (B) have a TPI of 10 and DR 1, and the yarns in (C) have a medium FC and TPI of 10.

Including a dye in the electrospinning solution allows for the visualization of fibers so that the fibers spun from two different solutions can be distinguished. Figure 2E visualizes different regions of a yarn under CLSM. The left end of the yarn has a green fluorescence because its fibers were dyed with DiO. The right end of the yarn has red fluorescence indicating the presence of DiI. When switching the dyed PCL solution during spinning, there is an area where both DiO and DiI dyed fibers overlap. This is shown in the middle section of the fiber where green and red fibers are present, and the two different fiber types are twisted together. The purpose of combining two differently dyed yarn segments is to demonstrate the ability to fabricate yarns with varying processing parameters at different segments. The middle section also demonstrates the ability to fabricate a yarn containing two different types of fibers. In this case, the parameter was a dye. A future goal is to fabricate yarns with segments of varying properties such as type of polymer, FC, twist, or DR.

3.2. Mechanics

Figure 3E–G presents the average tenacity of PCL MFTY fabricated with different manufacturing parameters. One manufacturing parameter was varied in each of the graphs: FC, TPI, and filament DRs. The parameter of interest was varied while the remaining parameters were kept constant (The only exception is NDR4 yarns which were fabricated using fibers spun from a 16% wt/v PCL solution). All manufacturing parameters influenced the yarn's tenacity and, subsequently, other mechanical properties. An increase in filament count resulted in an increase in tenacity. High filament count yarns had the tenacity of $125e^3$ Nm kg^{-1} compared to $106e^3$ and $64e^3$ Nm kg^{-1} for medium and low filament count yarns. Increasing the DR of the fibers making up the yarns also resulted in an increase in yarn tenacity with yarns fabricated from DR = 2.5 fibers having a higher tenacity than yarns fabricated using DR = 1 fibers. However, NDR4 yarns had a lower tenacity than yarns with a DR of 2.5. Varying the TPI demonstrated a different trend with an increase in tenacity being observed as TPI was increased from 10 to 20. Average tenacity decreased for yarns spun at 40 and 80 TPI compared to yarns spun at 20 TPI. However, both 40 and 80 TPI yarns had a higher average tenacity than yarns spun at 10 TPI. The same trends were observed for the UTS as both tenacity and UTS are closely related quantities.

An increase in the elastic modulus was observed as FC increased ranging between 282 and 323 MPa. A nonlinear relationship was observed when varying TPI. Elastic modulus

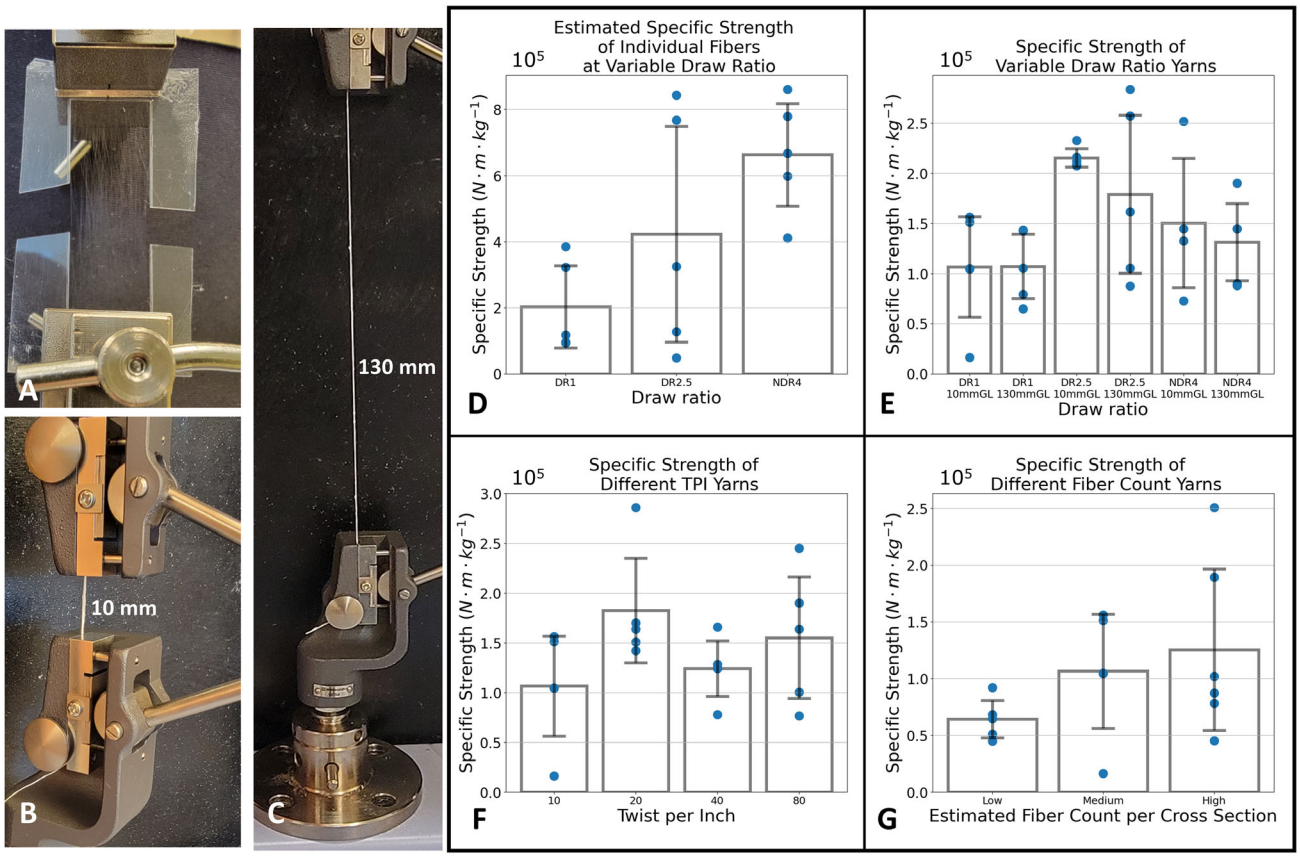

Figure 3. A–C) Experimental setup for tensile testing A) PCL fibers and B,C) their twisted yarns with two different GL. D–G) Average specific strength (tenacity) in Nm kg^{-1} of individual PCL fibers and PCL yarns. D) Tenacity of individual PCL fibers at varying DRs. E) Tenacity of PCL yarns with varying DR and GL made with medium FC and 10 TPI. F) Tenacity of PCL yarns with varying TPI made with a medium FC and spun at DR 1. G) Tenacity of PCL yarns with varying FC made with 10 TPI and spun at DR 1. Unless specified all yarns had a testing GL of 10 mm. The large GL (130 mm) is greater than the length of a single fiber (12 cm).

Table 2. Summary of mechanical properties of PCL yarns manufactured with different parameters. The FC category was spun at DR = 1 and TPI = 10. The TPI category was spun at DR = 1 and medium FC. The DR category was spun at TPI = 10 and medium FC (The asterisk is used to indicate that the DR4 group yarns were spun using a less concentrated spinning solution).

	Estimated [FC] per yarn cross section		Linear density [den]	Specific strength/tenacity [gf den^{-1}, Nm kg^{-1}]	UTS [MPa]	Elastic modulus [MPa]	Yarn-to-fiber strength ratio [%]
FC (TPI = 10) (DR = 1)	Low	2,047	54, $\sigma = 54$	0.73 (64 220)	73	282	32
	Medium	3411	90, $\sigma = 25.2$	1.21 (106 487)	122	303	53
	High	34 115	900, $\sigma = 25$	1.42 (125 403)	144	323	62
TPI (FC = Medium) (DR = 1)	20	10 234	270, $\sigma = 63$	2.07 (182 375)	209	323	90
	40	13 646	360, $\sigma = 106$	1.42 (124 169)	142	206	61
	80	9,211	245, $\sigma = 21.5$	1.76 (155 117)	177	161	77
DR (TPI = 10) (FC = Medium)	2.5	17 013	270, $\sigma = 63$	2.44 (215 281)	246	495	51
	4 *(16% solution)	89 367	396, $\sigma = 135$	2.00 (150 237)	200	234	23

increased to a maximum value of 323 MPa at TPI = 20. However, increasing TPI beyond 20 caused a decrease in the elastic modulus. The maximum elastic modulus value of 495 MPa was observed at DR 2.5

Statistical significance was analyzed using ANOVA and student's *t*-tests with the following results: ANOVA between the FC groups showed no statistical significance. *T*-tests also showed no significance between groups in group-to-group comparisons. ANOVA also showed no statistical difference between the TPI groups. However, *t*-tests showed statistical significance when comparing TPI of 10 and 20 ($p = 0.0351$), TPI 10 and 80 ($p = 0.0102$), and TPI 20 and 40 ($p = 0.043$). ANOVA was not performed on DR groups as only two groups were compared. *T*-test showed a significant difference between DR 1 yarns and DR 2.5 yarns ($p = 0.0013$). NDR4 fibers were not part of any statistical comparisons as they were made from a different spinning solution.

To summarize, increasing the FC, which is proportional to the linear density, resulted in an increase in tenacity, UTS, as well as the elastic modulus. The same increase was observed when increasing the DR of component fibers. Increasing the yarn twist from 10 to 20 TPI resulted in an increase of the aforementioned mechanical properties followed by a decrease in those properties for TPIs of 40 and 80. The values of the all the mechnical properties are summarized in **Table 2**. These results are consistent with the reported literature. Many reported studies demonstrated increased mechanical strength in yarn as the linear density is increased.[27–29] Additionally, many reported studies demonstrated that the overtwisting yarns could decrease their mechanical strength.[30–34]

4. Discussion

Current electrospun nanoyarn fabrication technology is confined to self-bundling or cone-spun yarns where little control is exerted over manufacturing parameters.[16] Another method deposits electrospun nanofibers into a vortexed water bath, which then twists fibers into a yarn.[35] An alternative nanoyarn fabrication method is described here, where electrospinning and yarn fabrication occur separately. Successful fabrication of MFTY was demonstrated using the proposed spinning device with a great degree of parameter control as shown in Figure 2A–C. SEM images show a demonstrable change of filament twist as the TPI control settings are changed (uptake motor speed and twist speed). TPI values were chosen to cover the same range of yarn twists common in the textile industry standards of low twist (10 TPI), medium twist (20 TPI), high twist (40 TPI), and very high twist (80 TPI).[36]

Expectedly, changing the manufacturing parameters resulted in a change in the mechanical properties of the MFTY. Two major factors play a role in the observed change in mechanical properties. First is the strength of the fibers making up the MFTY. This is dependent on the polymer backbone, crystallinity, and molecular alignment.[37] Increasing the DR of the polymer fiber increases the macromolecular alignment and tensile strength of the fiber. Figure 3D shows that individual PCL fibers with a DR of 2.5 are stronger than their DR 1 counterparts and fibers with a DR of 4 are the strongest fibers. This observation was also demonstrated in previous studies.[25] The previous factor is tied to the component fiber strength. However, yarn failure does not necessarily mean tensile failure of the component fibers. This leads us to the second factor that affects yarn mechanics, which is fiber-to-fiber friction. The yarn's structure is held together by the friction forces between the filaments. Friction can be increased by increasing the TPI as it allows for more filaments to interact with each other.[38] This is an example of static friction where a minimum force is needed for slippage to occur. These two factors were controlled using the three manufacturing parameters of filament count, DR, and TPI.

Increasing the DR results in better polymer chain alignment, which results in stronger fibers and, consequently, stronger yarns. This can be seen in Figure 3D–E. Increasing the DR and FC both resulted in an increase in the mechanical strength of yarns with a DR of 2.5 compared to yarns with a DR of 1. NDR4 yarns on the other hand were weaker than DR 2.5 yarns. At first glance, this is an unexpected result since NDR4 fibers are significantly stronger than DR 2.5 fibers. However, yarn mechanical failure does not mean fiber failure but is most likely due to slippage. Studies exploring the effect of fiber diameter on fiber surface properties have shown a decrease in surface roughness as the fiber diameter decreases.[39] A smoother surface results in lower fiber-to-fiber friction which leads to earlier slippage. This is a likely explanation for the drop in strength;

however, further investigation is needed to verify this finding. The effect of the decrease in surface roughness would have to outweigh the effect of the increased total surface area of NDR4 nanoyarns to result in the overall drop in strength.

Since tenacity describes the strength-to-weight ratio of a material, we expect tenacity to remain constant as FC increases. However, an increase was observed with increased FC. Further investigation into this correlation is needed, but we hypothesize that an increase in FC results in more fiber-to-fiber interactions that increase the strength-to-weight ratio.

Increasing the TPI in yarn allows for more individual filaments to interact with each other, which increases the total friction as more slippages need to occur for the yarn to fail. Figure 3F shows an increase in yarn strength when increasing the TPI from 10 to 20. However, yarn strength decreases for yarns with a TPI of 40 and 80. What is the mechanism behind this observation? TPI increases fiber-fiber friction as the yarns with 20 TPI demonstrated a higher mechanical strength than their 10 TPI counterpart. For TPIs > 20, we suspect that the friction force increases as well. However, overtwisting of the yarn may result in the filaments weakening. Thus, we suspect that fiber breakage or deformation has a greater contribution to yarn failure than filament slippage for yarns of TPI > 20. Other published papers studying yarn twists arrived at the same conclusion as well.[32,33]

Failure due to slippage means that yarns are typically weaker than their individual filaments under tensile load. For example, a single cotton fiber could have a tenacity of 3 gf den^{-1} while its twisted yarn made from the same fibers could have a tenacity of 1 gf den^{-1}. As a result, it is useful to look at the strength ratio of yarn-versus-fiber as it could be a good indicator of the usability of certain materials as a yarn. At medium filament count and a TPI of 10, both DR groups (DR 1 and DR 2.5 and medium FC) had a yarn-to-filament strength ratio of ≈50%. Importantly, this characteristic was conserved when the tensile testing GL was 130 mm, which is slightly larger than the length of the component fibers. NDR4 yarns had an ≈22% yarn-to-fiber strength ratio. The reason behind this is that NDR4 fibers are significantly stronger than both DR1 and DR2.5 fibers. Achieving a higher yarn-to-filament strength ratio will require much stronger friction forces between the component fibers.

One of the goals of this project is to fabricate electrospun yarns with mechanical properties of high quality as compared against the current state of the art in both the electrospun yarn manufacturing space, and the conventional staple yarn manufacturing space. High-tenacity MFTYs were successfully produced with a maximum tenacity of 2.44 gf den^{-1}. Conventional staple yarns can be made in a variety of ways using many materials. Some of the materials used in conventional yarn manufacturing are natural ones like cotton, wool, flax, and silk as well as synthetic ones such as polyester, polypropylene (PP), and nylon.[40–43] It is also worth noting that comparison will be limited to single-ply yarns as all the PCL MFTYs produced in this study were single-ply. 61/1 ring-spun cotton yarn has been reported to have a tenacity of 1.56 gf den^{-1}.[44] This is similar to the tenacity of all the MFTYs produced in this study. However, cotton yarn production method and processing parameters also affect its tenacity.[45] Reported cotton yarn tenacities have a range of 0.31–5.98 gf den^{-1}.[46] Studies testing cotton have also shown that the tenacity of cotton yarn ranges between 31 and 37% of the tenacity of its filaments.[29] PCL MFTYs had a tenacity ratio of 50% for both DR1 and DR2.5 fiber yarns, which demonstrates an increase in yarn-to-filament strength ratio compared to cotton yarns. Another popular conventional textile material is wool, which has a reported tenacity of 0.98–1.67 gf den^{-1},[46] which puts wool yarns on a comparable strength of PCL MFTYs. For yarn-to-fiber tenacity ratio, PCL MFTYs also outperformed wool, which has a tenacity ratio of 25–33%[47] compared to the PCL MFTY's 50%. It is also interesting to compare PCL MFTYs' mechanical performance to synthetic continuous filament yarns such as PP, which would be expected to be much stronger. It has been reported that melt-spun PP yarns of DR 7.3 had a tenacity of 7.2 gf den^{-1} compared to DR 3.73 which had a tenacity of 2.93 gf den^{-1}.[28] It is worth noting that PCL MFTYs of DR 2.5 were only 16.4% weaker compared to the PP yarns of DR 3.73, despite the reported bulk tenacity of PCL being around 0.3 gf den^{-1}[48] compared to 0.5 gf den^{-1} for PP.[49] These comparisons demonstrate that long polymer MFTY can be manufactured with mechanical strength comparable to conventional natural staple yarns and synthetic continuous yarns.

Self-bundling electrospun nanoyarns have been made using a wide variety of polymers such as polylactic acid (PLA), polyacrylonitrile (PAN), poly(vinylidene fluoride-*co*-hexafluoropropylene) (PVDF-HFP), PCL, and many more.[50] However, due to fiber fabrication and yarn spinning occurring simultaneously, fiber postprocessing, prior to yarn spinning, is rare and challenging. Tenacities of electrospun nanoyarns are reported in **Table 3**.[50] All the yarns reported in Table 3 were made using the self-bundling or cone spinning methods. No fiber postdrawing was performed prior to yarn spinning. However, PAN self-bundled yarns were melt-drawn postspinning by various DRs. Mechanics of pure AC electrospun yarns were not reported in the literature.[20,21]

For all reported polymers, higher twist and FC resulted in higher tenacity. Except for PAN, all the yarns reported in Table 3 were outperformed by at least one or more of the PCL MFTYs. Moreover, the tenacities of most yarns in these studies were at the lower end of their respective reported ranges. For example, six out of the seven reported tenacities of self-bundling and cone-spun PCL were less than or equal to 0.05 gf den^{-1},[34,51] while 25 out of the 32 reported tenacities of self-bundling and cone-spun PAN were less than or equal to 1.0 gf den^{-1}.[34,52–59]

Next, we analyze how manufacturing parameters affected the elasticity of MFTYs. Previous work on cotton and wool yarn showed no clear trend between FC and the elastic modulus of the yarn.[60] Twist also had no effect on elasticity for cotton yarns, as well as wool and wool–polyester (PE) blends.[47,61] When it comes to synthetic polymer yarns, previous work shows minimal changes in the elastic modulus as FC increases for PE yarns.[62]

Table 3. Reported tenacities of self-bundling and cone-spun electrospun nanoyarns of various polymers compared to parallel track manufactured PCL MFTYs.

Polymer	PLA[63]	PCL[34,51]	PVDF-HFP[64]	PAN[34,52–59]	PCL MFTYs
Tenacity [gf den^{-1}]	0.017–0.11	0.015–0.41	0.0267–0.097	0.04–3.55	0.73–2.44

However other studies have shown a decrease in the elastic modulus for high twist yarns.[32,33] For PCL MFTYs, statistically insignificant differences were observed in the average elastic modulus when FC was varied. For PCL MFTYs, twist resulted in no significant change in the elastic modulus when comparing yarns with TPI = 10 and yarns with TPI = 20. However, a significant decrease in elastic modulus is observed when TPI increases beyond 20.

A future goal is to produce uniform nanoyarns of commercially desirable length and to produce nanoyarns with segments of varying properties along the length of the yarn. Since this manufacturing approach is polymer-agnostic, nanoyarns can be made of other polymers such as PAN, PLA, and PVDF. This will allow the use of MFTY's in many application spaces such as medical sutures, sensors, and performance or smart textiles. One of the major limitations of the methodology presented in this study is the low production output. However, we expect that this collector-based technology will be compatible with numerous approaches to increase electrospinning throughput that are described in the literature, such as multineedle, needleless, and gas-assisted electrospinning.

5. Conclusion

A novel yarn fabrication process was utilized to produce PCL MFTY with good control over manufacturing parameters. Production of long yarns (>1 m), without significant reductions in strength, indicates the potential to scale up the process to produce commercial-scale continuous yarns at lengths of hundreds of meters. Varying manufacturing parameters affected the strength of the yarns' component fibers as well as fiber-to-fiber interactions which in turn affected the tenacity of the yarn. Increasing fiber draw and count increased the tenacity of the resulting yarn, while overtwisting resulted in a decrease in tenacity.

Supporting Information

Supporting Information is available from the Wiley Online Library or from the author.

Acknowledgements

This study was funded by the National Science Foundation (NSF) PFI-TT grant 2345785.

Conflict of Interest

The authors declare no conflict of interest.

Author Contributions

Mohamad Keblawi: conceptualization (equal); data curation (lead); formal analysis (lead); methodology (lead); validation (equal); visualization (lead); writing—original draft (lead); writing—review & editing (equal). **Adaugo Enuka**: data curation (supporting); investigation (supporting); writing—original draft (supporting). **Darrian Shufford**: investigation (supporting); methodology (supporting). **Vince Beachley**: conceptualization (equal); funding acquisition (lead); project administration (lead); supervision (lead); validation (equal); writing—review & editing (equal).

Data Availability Statement

The data that support the findings of this study are available from the corresponding author upon reasonable request.

Keywords

electrospinning, nanofiber, nanofiber yarns, polymer

Received: August 9, 2024
Revised: January 30, 2025
Published online: February 26, 2025

[1] S. Grishanov, in *Handbook of Textile and Industrial Dyeing* (Ed: M. Clark), Woodhead Publishing, Swaston, Cambridge **2011**, pp. 28–63.
[2] M. Okamoto, in *Advanced Fiber Spinning Technology* (Eds: T. Nakajima, K. Kajiwara, J.E. McIntyre), Woodhead Publishing, Swaston, Cambridge **1994**, pp. 187–207.
[3] P. Bhat, A. Basu, in *Advances in Silk Science and Technology* (Ed: A. Basu), Woodhead Publishing, Swaston, Cambridge **2015**, pp. 121–140.
[4] P. R. Lord, in *Handbook of Yarn Production* (Ed: P. R. Lord), **2003**, Woodhead Publishing, Swaston, Cambridge pp. 1-17.
[5] X. Chen, in *Computer Technology for Textiles and Apparel* (Ed: J. Hu), Woodhead Publishing, Swaston, Cambridge **2011**, pp. 93–121.
[6] I. A. Elhawary, in *Textiles and Fashion* (Ed: R. Sinclair) **2015**, Woodhead Publishing, Swaston, Cambridge pp. 191-212.
[7] D. A. J. Brennan, D. Jao, M. C. Siracusa, A. R. Wilkinson, X. Hu, V. Z. Beachley, *Polymer* **2016**, *103*, 243.
[8] P. E. Sasser, F. M. Shofner, Y. T. Chu, C. K. Shofner, M. G. Townes, *Text. Res. J.* **1991**, *61*, 681.
[9] F. Fadil, N. D. N. Affandi, M. I. Misnon, N. N. Bonnia, A. M. Harun, M. K. Alam, *Polymers* **2021**, *13*, 2087.
[10] J. Xue, T. Wu, Y. Dai, Y. Xia, *Chem. Rev.* **2019**, *119*, 5298.
[11] D. Kai, S. S. Liow, X. J. Loh, *Mater. Sci. Eng. C* **2014**, *45*, 659.
[12] D. Lv, M. Zhu, Z. Jiang, S. Jiang, Q. Zhang, R. Xiong, C. Huang, *Macromol. Mater. Eng.* **2018**, *303*, 1800336.
[13] J. Li, X. Zhang, Y. Lu, K. Linghu, C. Wang, Z. Ma, X. He, *Adv. Fiber Mater.* **2022**, *4*, 108.
[14] C. Li, M. Qiu, R. Li, X. Li, M. Wang, J. He, G. Lin, L. Xiao, Q. Qian, Q. Chen, J. Wu, X. Li, Y.-W. Mai, Y. Chen, *Adv. Fiber Mater.* **2022**, *4*, 43.
[15] L. Zhan, J. Deng, Q. Ke, X. Li, Y. Ouyang, C. Huang, X. Liu, Y. Qian, *Adv. Fiber Mater.* **2022**, *4*, 203.
[16] D. Kamireddi, R. M. Street, C. L. Schauer, *Polym. Eng. Sci.* **2023**, *63*, 677.
[17] I. Borazan, *J. Text. Inst.* **2023**, *114*, 1918.
[18] İ. Borazan, A. Celik Bedeloglu, *J. Appl. Polym. Sci.* **2024**, *141*, e54948.
[19] A. S. Levitt, C. E. Knittel, R. Vallett, M. Koerner, G. Dion, C. L. Schauer, *J. Appl. Polym. Sci.* **2018**, *135*, 46404.
[20] P. Pokorny, E. Košťáková, F. Sanetrník, P. Mikeš, T. Kalous, M. Bílek, K. Pejchar, J. Valtera, D. Lukáš, *Phys. Chem. Chem. Phys.* **2014**, *16*, 26816.
[21] S. Maheshwari, H.-C. Chang, *Adv. Mater.* **2009**, *21*, 349.
[22] A. A. Conte, K. Sun, X. Hu, V. Z. Beachley, *Front. Chem.* **2020**, *8*, 610.

[23] S. Wu, J. Liu, J. Cai, J. Zhao, B. Duan, S. Chen, *Biofabrication* **2021**, *13*, 045018.
[24] S. Nauman, G. Lubineau, H. F. Alharbi, *Membranes* **2021**, *11*, 39.
[25] D. A. Brennan, K. Shirvani, C. D. Rhoads, S. E. Lofland, V. Z. Beachley, *MRS Commun.* **2019**, *9*, 764.
[26] N. Haleem, X. Wang, *Text. Res. J.* **2015**, *85*, 211.
[27] A. H. Alias, P. M. Tahir, K. Abdan, M. S. Sapuan, M. S. Wahab, M. P. Saiman, *Sains Malays.* **2018**, *47*, 1853.
[28] A. Vitkauskas, R. Miglinaitė, P. Vesa, A. Puolakka, *Work* **2005**, *4*, 0.6.
[29] H. Ramey Jr., R. Lawson Jr., S. Worley Jr., *Text. Res. J.* **1977**, *47*, 685.
[30] S. F. Fennessey, R. J. Farris, *Polymer* **2004**, *45*, 4217.
[31] I. Mertová, E. Moučková, B. Neckář, M. Vyšanská, *Autex Res. J.* **2018**, *18*, 110.
[32] T. Kitao, J. E. Spruiell, J. L. White, *Polym. Eng. Sci.* **1979**, *19*, 761.
[33] J. C. Anike, K. Belay, J. L. Abot, *Carbon* **2019**, *142*, 491.
[34] A. S. Levitt, C. E. Knittel, R. Vallett, M. Koerner, G. Dion, C. L. Schauer, *J. Appl. Polym. Sci.* **2017**, *134*.
[35] A. Sensini, L. Cristofolini, *Materials* **2018**, *11*, 1963.
[36] S. J. Kadolph, in *Textiles*, 10th ed., Pearson Prentice Hall, Upper Saddle River, NJ **2007**.
[37] M. D. Flamini, T. Lima, K. Corkum, N. J. Alvarez, V. Beachley, *Mater. Adv.* **2022**, *3*, 3303.
[38] D. U. Shah, P. J. Schubel, M. J. Clifford, *J. Compos. Mater.* **2013**, *47*, 425.
[39] H. H. Kim, M. J. Kim, S. J. Ryu, C. S. Ki, Y. H. Park, *Fibers Polym.* **2016**, *17*, 1033.
[40] B. Das, S. Ishtiaque, R. Rengasamy, *Res. J. Text. Apparel* **2011**, *15*, 70.
[41] A. Anghileri, G. Freddi, R. Mossotti, R. Innocenti, *J. Nat. Fibers* **2007**, *4*, 13.
[42] L. Yan, N. Chouw, K. Jayaraman, *Composites Part B* **2014**, *56*, 296.
[43] Y. E. Elmogahzy, in *9-Yarns, In Engineering Textiles* (Ed: Y.E. Elmogahzy), 2nd ed., Woodhead Publishing, Swaston, Cambridge **2020**, pp. 223–248.
[44] J. Peterson, A. Eckard, J. Hjelm, H. Morikawa, *J. Nat. Fibers* **2021**, *18*, 492.
[45] T. Jackowski, B. Chylewska, D. Cyniak, *Fibres Text. East. Eur.* **2002**, *10*, 27.
[46] M. J. Smith, T. H. Flowers, F. J. Lennard, *Stud. Conserv.* **2015**, *60*, 375.
[47] D. Jankowska, A. Wyrostek, B. Patkowska–Sokoła, K. Czyż, *J. Nat. Fibers* **2021**, *18*, 1512.
[48] K. Ragaert, I. De Baere, L. Cardon, J. Degrieck, in *6th Polymers & Mould Innovations Int. Conf.* **2014**.
[49] W. D. Callister, D. G. Rethwisch, in *Fundamentals of Materials Science and Engineering*, Vol. *471660817*, Wiley, London **2000**.
[50] F. Göktepe, B. B. Mülayim, *Autex Res. J.* **2018**, *18*, 87.
[51] L. A. Bosworth, *Conference Papers in Science*, Wiley Online Library, Birmingham, UK **2014**.
[52] C.-I. Su, T.-C. Lai, C.-H. Lu, Y.-S. Liu, S.-P. Wu, *Fibers Polym.* **2013**, *14*, 542.
[53] J. X. He, K. Qi, Y.-M. Zhou, S.-Z. Cui, *Polym. Int.* **2014**, *63*, 1288.
[54] S. Wu, Y. Zhang, P. Liu, X. Qin, *Text. Res. J.* **2016**, *86*, 1716.
[55] S.-H. Wu, X.-H. Qin, *Mater. Lett.* **2013**, *106*, 204.
[56] F. Dabirian, A. H. Seyed Ravandi, R. H. Sanatgar, J. P. Hinestroza, *Fibers Polym.* **2011**, *12*, 610.
[57] X. Wang, K. Zhang, M. Zhu, B. S. Hsiao, B. Chu, *Macromol. Rapid Commun.* **2008**, *29*, 826.
[58] J. He, Y. Zhou, K. Qi, L. Wang, P. Li, S. Cui, *Fibers Polym.* **2013**, *14*, 1857.
[59] J. He, K. Qi, Y. Zhou, S. Cui, *J. Appl. Polym. Sci.* **2014**, *131*, 40137.
[60] H. Ahmed, *Int. Des. J.* **2020**, *10*, 103.
[61] R. Dhingra, S. De Jong, R. Postle, *Text. Res. J.* **1981**, *51*, 759.
[62] T. S. Lemmi, M. Barburski, A. Kabziński, K. Frukacz, *Materials* **2021**, *14*, 1666.
[63] A. M. Afifi, S. Nakano, H. Yamane, Y. Kimura, *Macromol. Mater. Eng.* **2010**, *295*, 660.
[64] U. Ali, Y. Zhou, X. Wang, T. Lin, *J. Text. Inst.* **2012**, *103*, 80.